

See discussions, stats, and author profiles for this publication at: <https://www.researchgate.net/publication/26666901>

# Cytosolic accumulation of HPV16 E7 oligomers supports different transformation routes for the prototypic viral oncoprotein: The amyloid-cancer connection

ARTICLE *in* INTERNATIONAL JOURNAL OF CANCER · OCTOBER 2009

Impact Factor: 5.09 · DOI: 10.1002/ijc.24579 · Source: PubMed

CITATIONS

19

READS

21

## 7 AUTHORS, INCLUDING:



**Leonardo Alonso**

Fundación Instituto Leloir

29 PUBLICATIONS 447 CITATIONS

[SEE PROFILE](#)



**Eduardo M Castaño**

Fundación Instituto Leloir

104 PUBLICATIONS 5,332 CITATIONS

[SEE PROFILE](#)



**Laura Morelli**

Fundación Instituto Leloir

57 PUBLICATIONS 2,039 CITATIONS

[SEE PROFILE](#)



**Gonzalo de Prat-Gay**

Fundación Instituto Leloir

96 PUBLICATIONS 1,817 CITATIONS

[SEE PROFILE](#)

## Cytosolic accumulation of HPV16 E7 oligomers supports different transformation routes for the prototypic viral oncoprotein: The amyloid–cancer connection

Karina Dantur<sup>1</sup>, Leonardo Alonso<sup>1</sup>, Eduardo Castaño<sup>1</sup>, Laura Morelli<sup>1</sup>, Juan Manuel Centeno-Crowley<sup>1</sup>, Susana Vighi<sup>2</sup> and Gonzalo de Prat-Gay<sup>1\*</sup>

<sup>1</sup>*Instituto Leloir and Instituto de Investigaciones Bioquímicas Buenos Aires, Conicet, Patricias Argentinas 435, (C1405BWE) Ciudad Autónoma de Buenos Aires, Argentina*

<sup>2</sup>*Departamento de Patología, Hospital de Clínicas, Universidad de Buenos Aires, Argentina*

E7 is the major transforming activity in human papillomaviruses, a causal agent for cervical cancer. HPV16 E7 is a small protein with a natively unfolded domain for which dozens of specific cellular targets were described, and represents a prototypical oncoprotein among small DNA tumor viruses. The protein can form spherical oligomers with amyloid-like properties and chaperone activity. Conformation specific antibodies locate endogenous oligomeric E7 species in the cytosol of 3 model cell lines, strongly colocalizing with amyloid structures and dimeric E7 localizes to the nucleus. The cytosolic oligomeric E7 appear as the most abundant species in all cell systems tested. We show that nuclear E7 levels are replenished dynamically from the cytosolic pool and do not result from protein synthesis. Our results suggest that long-term events related to de-repression of E7 would cause accumulation of excess E7 into oligomeric species in the cytosol. These, together with the known target promiscuity of E7, may allow interactions with many of the non-pRb dependent targets described. This hypothesis is further supported by the detection of E7 oligomers in the cytosol of cancerous cells from tissue biopsies.

© 2009 UICC

**Key words:** cancer; oncoprotein; papillomavirus; E7; amyloid

Small DNA tumor viruses share the requirement of the cellular DNA replication machinery to amplify their genome when they must force cells into the S phase.<sup>1</sup> The main proteins behind the cell transforming activity are E1A in adenovirus, large T-antigen in SV40 and the E7 oncoprotein in papillomavirus.<sup>2</sup> Although the large T-antigen polypeptide is multidomain and multifunctional, the papillomavirus E7 protein is small with not known biochemical functions other than protein–protein interactions. Besides sequence homology, they also share the property of sequestering and destabilizing the retinoblastoma (pRb) family of proteins, which are essential tumor suppressors that regulate the cell cycle.<sup>3–5</sup>

Human papillomaviruses (HPV) infect epithelia and are causal agents for benign and malignant diseases, where the most widespread is cervical cancer in women.<sup>6</sup> Two virus-like particle-based vaccines proved to be highly efficacious for preventing the infection.<sup>7</sup> However, these vaccines are prophylactic and there is still the need of treatment of the female world population between 15 and 75 years old and, with 5 million estimated cancer deaths over the next 20 years due to existing HPV infections.<sup>8</sup>

Of the 8 proteins that are encoded by its small 8 kb DNA genome, 2 proteins, E6 and E7 cooperate for transformation by HPV.<sup>9,10</sup> The primary events behind transformation by E6 is binding and degradation of p53.<sup>11</sup> Similarly, E7 was early described to bind pRb,<sup>10</sup> promoting its degradation via the ubiquitin proteasome system,<sup>12</sup> with counterparts in other DNA tumor viruses, thus validating a common strategy.<sup>13</sup> However, E7 is the major transforming protein in HPV, since its interaction with hypophosphorylated pRb causes disruption of growth-suppressive pRb-E2F complexes that play important roles in the regulation of the G1/S-phase transition.<sup>11,12</sup>

A wide variety of binding partners have been and continue to be identified, suggesting multiple ways by which E7 may induce transformation and subsequent progression into cancer.<sup>14</sup> Immunofluorescence microscopy studies have reported that HPV16 E7 is predominantly nuclear in the cervical cancer cell line CaSki and

in experimental human cell lines transiently expressing it.<sup>15,16</sup> In cancer cervical biopsies, E7 was predominantly detected in the nucleus of the tumor cells.<sup>15,16</sup> E7 has a relatively short half-life in CaSki cells and its degradation is mediated by the ubiquitin–proteasome pathway through its N-terminus.<sup>17,18</sup>

The oncoprotein is an extended dimer<sup>19,20</sup> with pH-dependent conformational transitions leading to differential exposure of hydrophobic surfaces, which we proposed could be related to its ability to bind different proteins.<sup>21,22</sup> We showed that HPV E7 can self-assemble into soluble and highly stable spherical oligomers (E7SOs) of 50 nm diameter and 790 kDa,<sup>23</sup> which displayed chaperone-holdase activity for model but unrelated chaperone substrate proteins.<sup>24</sup> The E7SOs were able to bind pRb with high avidity, since they are multivalent with respect to the LXCXE motif.<sup>23</sup> These oligomers showed amyloid-like properties, as judged by their ability to bind congo red and thioflavin-T dyes.<sup>23</sup>

Given the ability of E7 to form oligomer with amyloid characteristic and chaperone-holdase activity, we set out to investigate the existence and localization of such conformers in established prototypic and transiently transfected human cell lines in search for a correlation with the transforming activity of E7. We were able to localize E7SOs in the cytosol, which co-localized with amyloid structures, in equilibrium with dimeric-monomeric forms that localized to the nucleus. In addition, we confirmed the presence of oligomeric forms of E7 in the cytosol of cells from HPV-linked cancerous tissue.

### Material and methods

#### Plasmids and reagents

The HPV-16 E7 sequence was amplified from the HPV-16 genome and inserted into BamHI and EcoRI sites of the pcDNA3 expression plasmid (Invitrogen, Buenos Aires, Argentina). All culture media and supplements were purchased from Invitrogen.

#### Cell culture and transfection

CaSki cells, derived from HPV16-positive human cervical cancer; U-2 OS, the non-HPV human osteosarcoma cell line and TC-1 mouse cell line, were obtained from the American Type Culture Collection (ATCC).

Additional Supporting Information may be found in the online version of this article.

**Abbreviations:** DAB, 3,3'-diaminobenzimide; E7m-d, E7 monomer–dimer; E7SOs, E7 soluble spherical oligomers; HPV, Human papillomavirus; ON, overnight; pRb, retinoblastoma protein; PVDF, polyvinylidene difluoride; TBS, Tris Buffer Saline; Tx100, TritonX 100.

Grant sponsor: ANPCyT; Grant number: PICT 01-10944; Grant sponsor: ICGBE; Grant number: CRP ARG0102.

**\*Correspondence to:** Instituto Leloir and Instituto de Investigaciones Bioquímicas Buenos Aires, Conicet, Patricias Argentinas 435, (C1405BWE) Ciudad Autónoma de Buenos Aires, Argentina.

Fax: 54-11-5238-7501. E-mail: gpg@leloir.org.ar

Received 9 March 2009; Accepted after revision 5 May 2009

DOI 10.1002/ijc.24579

Published online 18 May 2009 in Wiley InterScience (www.interscience.wiley.com).

CaSki, U-2 OS and TC-1 cell lines were grown in Dulbecco's modified Eagle medium (DMEM) supplemented with 10% FBS, antibiotic-antimycotic and glutamine. U-2 OS cells were transiently transfected at 60% confluence with the pcDNA3-HPV-16 E7 expression plasmid using GeneJuice Transfection Reagent (Novagen, Merck, Argentina). pcDNA3-EGFP was cotransfected together with pcDNA3-E7 to control the transfection efficiency.

#### *Polyclonal anti-HPV-16 E7 antibodies*

BALB/c mice were immunized intraperitoneally with purified soluble HPV-16 E7<sub>m-d</sub> protein in complete Freund's adjuvant, and standard procedures were followed. In another immunization plan, we obtained polyclonal anti-HPV-16 E7 SOs antibodies using highly purified E7SOs proteins as immunogen. For cleaner results, the  $\gamma$ -globulin fraction was enriched by ammonium sulphate precipitation. Spleenocytes obtained from the immunized mice with E7SOs were fused with a NS0 mouse plasmocytoma cell line following established techniques.<sup>25</sup> From all the screened hybridoma supernatants, the monoclonal antibody IgG M1 displayed high reactivity against the E7 protein. The affinity of this monoclonal for HPV16 E7 is in the low nanomolar range and will be described elsewhere.

#### *Immunofluorescence analysis*

CaSki, U-2 OS and TC-1 cells were grown overnight (ON) on glass cover slips to ~60% confluence and fixed with cold methanol for 5 min at -20°C. Subsequently, cells were blocked and permeabilized with 0.1% gelatin from bovine skin, type B (Sigma-Aldrich, Argentina) and 0.1% Triton X-100 in PBS for 30 min at room temperature. Cells were incubated with the obtained anti-E7<sub>m-d</sub> and anti-E7SOs polyclonal or the monoclonal M1 anti-E7 antibodies, 2 hr at RT in blocking solution. The cells were then incubated for 1 hr with Cy3-labeled donkey anti-mouse IgG antibody (Jackson ImmunoResearch, Baltimore, US). The coverslips were mounted with Mowiol 4-88 reagent (Calbiochem, Merck, Argentina). As negative controls, parallel sets of slides were incubated with either preimmune serum instead of primary polyclonal antibodies or avoiding the primary antibody for monoclonal.

Immunoneutralization experiments were carried out by preincubating the polyclonal or monoclonal anti-E7 antibodies with 1 mg/ml solution of purified HPV-16 E7<sub>m-d</sub> or with HPV-16 E7SOs conformers, for 1 hr at RT.

For amyloid staining procedure, 0.005% thioflavin-S dye (Sigma) was added after washing the cells extensively with PBS and then incubating for 10 min with the fluorescent dye. Next, the cells were washed 3 times in 70% ethanol and once in water before mounting. Co-localization analysis of the images was carried out using the Zeiss LSM image browser software (Fig. 2, Supporting Information). Images were obtained in an LSM 510 PAS-CAL confocal microscope (Carl Zeiss, Oberkochen, Germany).

#### *Proteasome and protein synthesis inhibition*

Cells were treated with DMSO or 10  $\mu$ M MG132 (Calbiochem) for 1, 3, 6, 9 and 12 hr. The protein half-life analysis for E7SOs was carried out by determining Cy3-labeled E7 fluorescence at various times in cell treated with the protein synthesis inhibitor cycloheximide (Sigma). Cells were collected at 0, 1, 3, 6 and 9 hr after treatment and processed for immunostaining, a fluorescence of 100% was attributed to cells collected at the 0 hr time-point. For E7SOs nuclear import experiments, CaSki cells were incubated with MG132 for 12 hr; after this incubation period, CHX was added together with fresh medium and MG132 for 3 hr. The media was subsequently removed and immediately replenished with CHX only. Cells were collected at times 3, 6 and 9 hr after CHX addition for immunofluorescence analysis.

#### *Immunoblotting*

Cells (~5  $\times$  10<sup>6</sup>) were lysed in buffer CHAPS (1% CHAPS in PBS, 2 mM MgCl<sub>2</sub>, 50  $\mu$ M MG132, 2 mM DTT, 2 mM PMSF and protease inhibitor cocktail from Sigma), for 30 min in ice, whole

cell extracts were centrifuged 5 min at 4000g, and nuclear pellet was resuspended in the same lysis buffer and sonicated for 3 sec. The total protein content was determined by Bradford assay. Equal amount of proteins (10  $\mu$ g) were loaded on a 15% SDS-polyacrylamide gel and transferred to a Hybond polyvinylidene difluoride (PVDF) membrane (Amersham Biosciences, Argentina, SA). Membranes were blocked in 3% BSA in tris buffer saline (TBS) overnight at 4°C, and subsequently incubated for 1.5 hr at RT with the anti-E7 monoclonal M1 antibody (dilution in 0.25% of BSA/TBS and 0.1% Tween 20). The membranes were analyzed with ECL plus system (Amersham Biosciences, Argentina, SA).

#### *Immunohistochemical detection of HPV16E7 in cervical biopsies*

Immunohistochemistry was performed on paraffin-embedded sections on 1 of the 3 DNA-HPV-16 positive endometrioid adenocarcinoma biopsies (see Supporting Information) and 1 non-HPV vaginal adenocarcinoma as a control (Fig. 4, Supporting Information). Ten-micrometer sections were mounted on slides, deparaffinized in xylene and hydrated in ethanol. Slides were then processed for antigen retrieval treatment with 100% formic acid. Endogenous peroxidase activity was blocked with 5% H<sub>2</sub>O<sub>2</sub>/cold methanol. Sections were washed with PBS-0.1% Triton-X 100 and incubated in blocking buffer (10% goat serum in PBS-0.1% Tx100). Slides were incubated with monoclonal M1, or gamma fraction anti-HPV16 E7SOs, rinsed in phosphate buffer pH 7.0, and incubated with the biotin or Cy3-conjugated anti-mouse IgG (Dako). After washing step, the samples were processed with an Avidin:Biotinylated enzyme Complex (VECTASTAIN ABC kit) following the manufacturer's instructions. Bound antibodies were visualized with DAB (3,3'-diaminobenzimide) as substrate chromogen or in Cy3 dye. The specimens were dehydrated with increasing concentrations of ethanol and xylene, and coverslipped using Canada Balsam solution.

## **Results**

#### *Detection and differential localization of E7 oligomers in cells*

The detection of conformers of E7 within cells required of antibody reagents with a high discrimination capacity. For this purpose, we analyzed the monoclonal antibody (M1) and the purified gamma fraction of 2 polyclonal mice antisera, raised against either E7 dimer or E7SOs (see Material and methods). The dissociation constant of E7 dimer in solution is weak (1  $\mu$ M),<sup>19</sup> and it is not possible to discriminate the state within the cell. For this reason, we refer to this species as E7 monomer-dimer (E7<sub>m-d</sub>). We labeled both E7<sub>m-d</sub> and E7SOs with fluorescein and followed fluorescence anisotropy changes as indicative of binding. While Figure 1C (Supporting Information) shows that the monoclonal does not discriminate both conformers in solution, the gamma fraction of the polyclonal sera raised against E7<sub>m-d</sub> can discriminate the latter from the oligomer. Moreover, the gamma fraction of the anti-E7SOs has the largest discrimination capacity between the 2 E7 conformers.

We next investigated the presence of the oligomers in HPV16 transformed CaSki cells. Staining with the anti-E7<sub>m-d</sub> gamma fraction shows a strong concentration of the label within the nucleus, and a mild labeling in the cytosol (Fig. 1a), in line with the cross-reactivity described in Figure 1A (Supporting Information). Selective immunoneutralization and precipitation of the anti-E7<sub>m-d</sub> with large excess of purified E7<sub>m-d</sub> prior to immunocytochemistry, eliminates nuclear labeling completely (Fig. 1b). In a similar experiment but using purified E7SOs instead for immunoneutralization, all label in the entire cell was eliminated, suggesting once again, that the anti-E7<sub>m-d</sub> displays substantial cross-reactivity compared to the anti-E7SOs reagent. In fact, the anti-E7SOs polyclonal evidences a strong and unequivocal cytosolic localization for the E7SOs (Fig. 1d). The very mild nuclear labeling is completely abolished by immunoneutralization of the anti-E7SOs with excess of E7<sub>m-d</sub>, leaving the nuclei completely devoid of label (Fig. 1e).

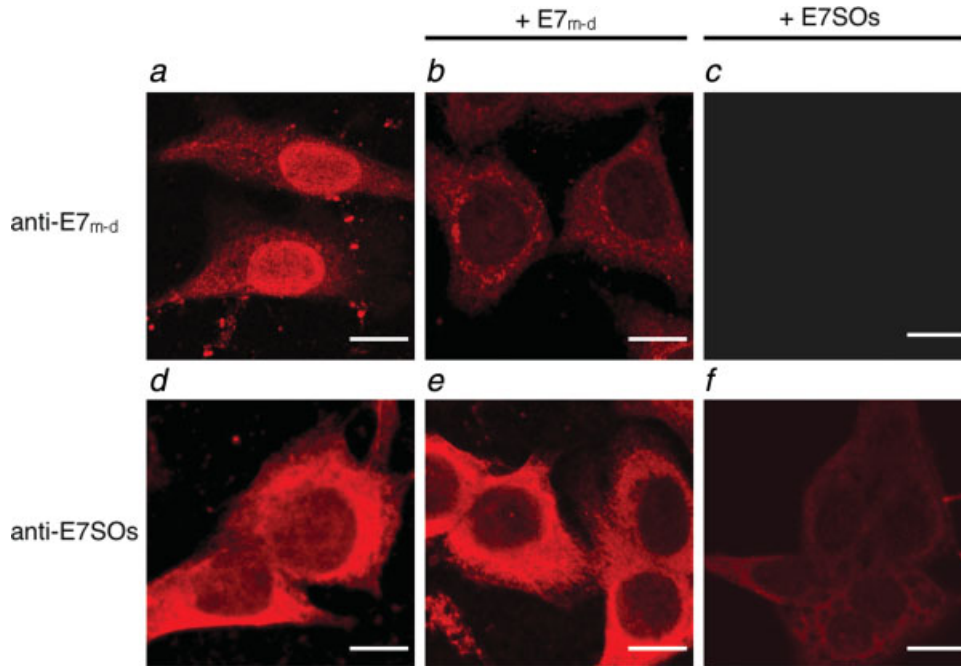


**FIGURE 1** – Discrimination of E7 conformers in CaSki cells. Fluorescence confocal microscopy CaSki cells, stained with the anti-E7<sub>m-d</sub> (a–c) or anti-E7SOs (d–f) purified gamma fractions. These were treated with an excess of highly purified and soluble HPV-16 E7<sub>m-d</sub> (b, e) and E7SOs (c, f) prior the immunofluorescence staining (see Material and methods) Bar: 10  $\mu$ m.

The human osteosarcoma derived U-2 OS cell line, transiently transfected with HPV16 E7, yielded identical results to the CaSki cells: the E7<sub>m-d</sub>, strongly localized in the nucleus and the E7SOs localized in the cytosol (Figs. 2a and 2b), both confirmed by immunoneutralization (not shown). The TC-1 cell line, widely used for challenge in therapeutic vaccination, is derived from a primary culture of a lung carcinoma stably transfected with HPV16 E6 and E7 oncoproteins, and the *H-ras* gene.<sup>26</sup> The anti-E7<sub>m-d</sub> antibody showed a strikingly defined nuclear localization of the signal, whereas the anti-E7SOs preferentially labeled the cytosol of TC-1 cells (Figs. 2c and 2d, respectively).

#### *Cytosolic E7 oligomers are the most abundant species*

We wanted to determine the ability of the monoclonal M1 to stain CaSki and transfected U-2 OS cells in comparison with the polyclonals. Immunofluorescence of CaSki cells stained with M1 showed a preferential staining of the cytosol (Fig. 3a), resembling what was observed with anti-E7SOs polyclonal (Fig. 1d). However, its neutralization by excess of E7<sub>m-d</sub>, suppressed the signal completely (Fig. 3b), unlike the case of anti-E7SOs in which only the nuclear species disappeared (Fig. 3b, inset and Fig. 1e). This result has 2 main interpretations. First, the epitope recognized by M1 is present in both E7<sub>m-d</sub>, and E7SOs. Second and rather important, is that given that the analysis is within a single experiment with the same antibody, the largely increased label in the cytosol strongly suggests that E7 preferentially accumulates as oligomers in this compartment.

Transfected U-2 OS cells yielded a pattern similar to CaSki cells (Fig. 3d). Neutralization by E7<sub>m-d</sub>, also abolished all signal (Fig. 3e), supporting the lack of discrimination of conformers and the accumulation of E7 in the cytosol. The overall preferential cytosolic labeling of E7 is evident in both CaSki and HPV16 E7 transfected U-2 OS cells (Figs. 3a and 3d, respectively).

To test for the presence of the E7 polypeptide, we analyzed the above mentioned cell lines by SDS-PAGE and western blot, using the monoclonal antibody M1 (Fig. 3g). The U-2 OS cells transfected with E7 and CaSki cells showed strong bands (lane 6 and 7, respectively), with weaker bands in SiHa (lane 3 and 4), expected from the low HPV genome copy number. The non-HPV cervical cancer cell line C33A was used as a negative control. It should be stressed that extracts had to be processed immediately after cell

lysis with MG132 and protease inhibitor cocktail, since otherwise E7 levels are not detectable due to its fast turnover.<sup>27</sup>

#### *Cytosolic E7 oligomers display amyloid conformation*

A salient feature of the E7SOs that we described *in vitro*, was its amyloid-like properties despite their soluble nature.<sup>23</sup> Since M1 detects both oligomeric and monomeric-dimeric forms, we used it as a single tool for detecting both species at the same time, and co-stained the cells with thioflavin-S in the same experiment. In CaSki cells, we observed the expected pattern for M1 with an increased cytosolic label, but lower amounts of E7<sub>m-d</sub> in the nucleus (Fig. 4a, compare to Fig. 3a). When the thioflavin-S label was analyzed, we found a strikingly similar pattern (Fig. 4b) which becomes more evident in the merge figure (Fig. 4c). Moreover, a clear co-localization of E7 and thioflavin-S dye was observed (Fig. 2, Supporting Information). E7 transfected U-2 OS cells displayed a similar behavior (Figs. 4d–4f). Finally, we co-stained the TC-1 E6/E7 containing tumor cell line, and confirmed the observed cytosolic amyloid-E7 co-localization pattern (Figures 4g–4i).

#### *Cytosolic presence of E7 oligomers in cervical biopsies of cancerous tissue*

We analyzed biopsies of tissue from an endometrioid adenocarcinoma positive for HPV16, together with non HPV carcinomas as control (Fig. 4, Supporting Information), using standard immunohistochemistry and the anti-E7 M1 monoclonal as the primary antibody. Figure 5A shows a low magnification field, where stroma (S), differentiated (D) and undifferentiated (U) regions in the tissue section are observable. Positive staining for E7 is clearly evident in the most differentiated papillar regions. Magnification of a positive region of the tissue shows a clear cytoplasmic localization (Fig. 5b), which parallels the alternative fluorescence staining using Cy3 labeled anti-mouse IgG (Figs. 5c and 5d).

In a parallel experiment, we stained the same tissue sample with anti-E7SOs as the primary antibody, and found an identical pattern (Fig. 5g). Close comparison at higher magnification indicates that both anti-E7 M1 monoclonal and anti-E7SOs locate the E7 label unequivocally in the cytosol (Figs. 5e vs. 5g). The same figures show a mild nuclear label for E7. The fact that the localization of E7 by the oligomer specific antibody and the M1 monoclonal



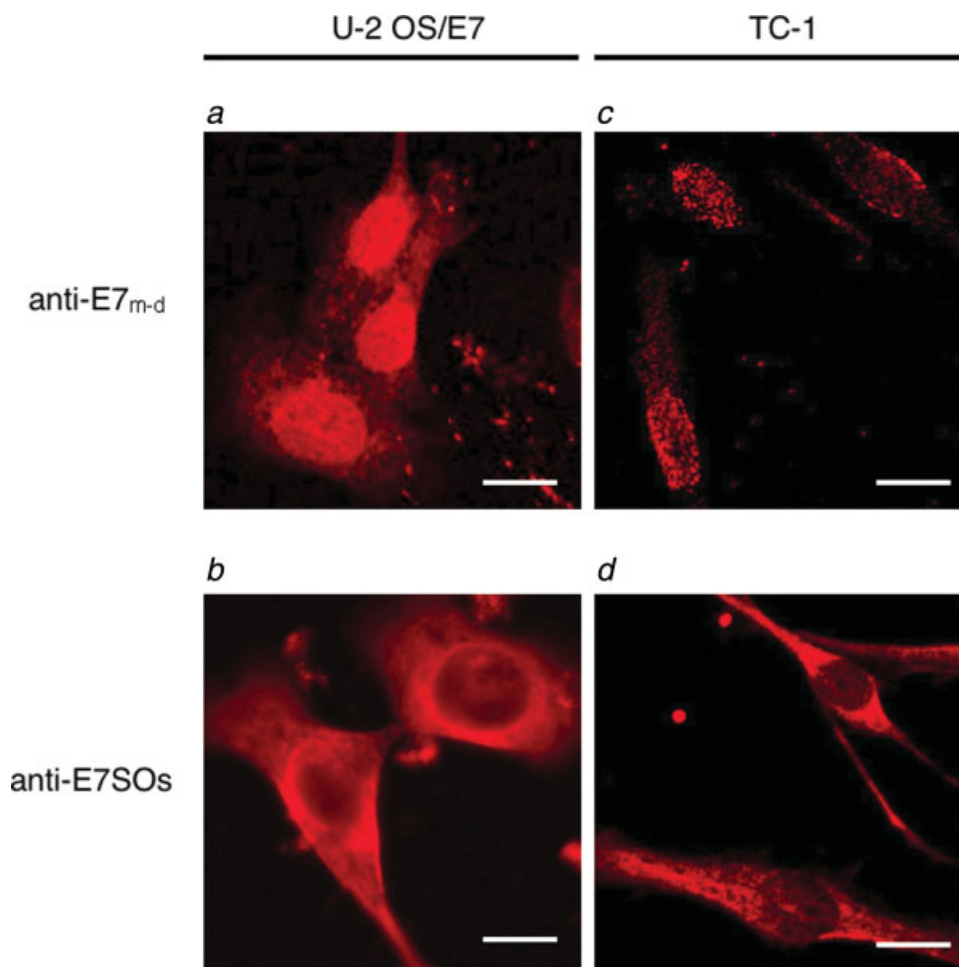


**FIGURE 2** – Differential localization of E7<sub>m-d</sub> and E7SOs in TC-1 cell line and E7 transfected U-2 OS. U-2 OS cells, transiently transfected with pCDNA3-HPV16 E7 (a, b), and TC-1 cell line (see text, c, d) were stained with anti-E7<sub>m-d</sub> (a, c) and with anti-E7SOs (b, d) purified gamma fractions from the respective polyclonal antisera. Bar: 10  $\mu$ m. [Color figure can be viewed in the online issue, which is available at [www.interscience.wiley.com](http://www.interscience.wiley.com).]

show a striking match, strongly suggests that the oligomeric forms of E7 are present in the cytosol of HPV linked cancerous tissue. No staining was observed during the immunodepletion experiment with both antibodies (Figs. 5f and 5h). These findings prove the high specificity of the anti-HPV-16 E7 antibodies.

#### *Nuclear E7<sub>m-d</sub> levels are restored at the expense of the cytosolic oligomeric E7 pool*

Since E7 is known to be degraded by the ubiquitin proteasome system,<sup>27,28</sup> we incubated CaSki cells with the 26S proteasome inhibitor MG132, and fixed them at different times for staining with anti-E7 M1. One hour after incubation, we observed no changes in the E7 distribution (Fig. 6a, 1 hr). This pattern was repeated at the third hour, which indicates the time it takes for the inhibitor to exert its full effect (Fig. 6a, 3 hr). At 6 hr, a marked increase of label was observed in the nucleus, more pronounced at 9 hr, where the pattern of labeling was inverted, with higher amounts of the nuclear E7<sub>m-d</sub> with respect to the cytosolic oligomers (Fig. 6a, 6 and 9 hr, respectively). This was the maximum effect attained with this inhibitor, since there were no changes in the localization pattern after 14 hr incubation. Thus, cytosolic oligomeric E7 can enter the nucleus when its degradation is blocked. To confirm this interpretation, our goal was to discriminate existing from *de novo* synthesized protein.

We designed an experiment where we blocked both proteasome degradation and protein synthesis. We incubated CaSki cells with both MG132 and cycloheximide, and observed the progression at same time periods (Fig. 6b). Similar to MG132 alone, there was little or no effect at 1 hr incubation (Fig. 6b, 1 hr). However, at 3

hr, there is a strong accumulation in the nucleus, and this accumulation occurred at the expense of a decrease in cytosolic label (Fig. 6b, 3 hr). After 6 hr incubation, the nuclear label was even more intense, and the cytosolic E7 disappeared completely (Fig. 6b, 6 hr). From 9 hr incubation onwards, the pattern was similar, but morphological changes in the cells became evident, most likely as a result of toxicity of the chemicals used (Fig. 6b, 9 hr). Altogether, these results indicate that the increase in nuclear accumulation of E7 due to proteasome inhibition is the product of the passage of cytosolic oligomeric E7 to the nucleus.

Cycloheximide alone inhibited E7 synthesis completely at 6 hr, leaving the oncoprotein undetectable by immunofluorescence (not shown). The complete disappearance of the protein from both cytosolic and nuclear compartments by cycloheximide treatment together with the accumulation of E7<sub>m-d</sub> in the nucleus by MG132 proteasome inhibition, strongly suggests that the degradation of E7 takes place mainly within the nucleus, and its levels are replenished from the cytosolic pool. In order to confirm this hypothesis, we pretreated CaSki cells for 14 hr to ensure complete proteasomal inhibition and maximum E7 accumulation in both cell compartments. We then added cycloheximide and, after a 3-hr incubation, washed the cells with cycloheximide only, to eliminate MG132 and release proteasome inhibition. The distribution pattern did not change for the first 3 hr, when the effect of the cycloheximide was only marginal (compare Fig. 6c, 3 hr with Fig. 6a, 9 hr). After 6 hr, when the effect of the inhibitor was maximum, the nuclear E7 was degraded first, and at 9 hr there was no detectable E7 (Fig. 6c, 9 hr). These results confirmed that the degradation of E7 occurs preferentially in the nucleus and that nuclear E7 levels are replenished dynamically from the cytosolic oligomeric pool.

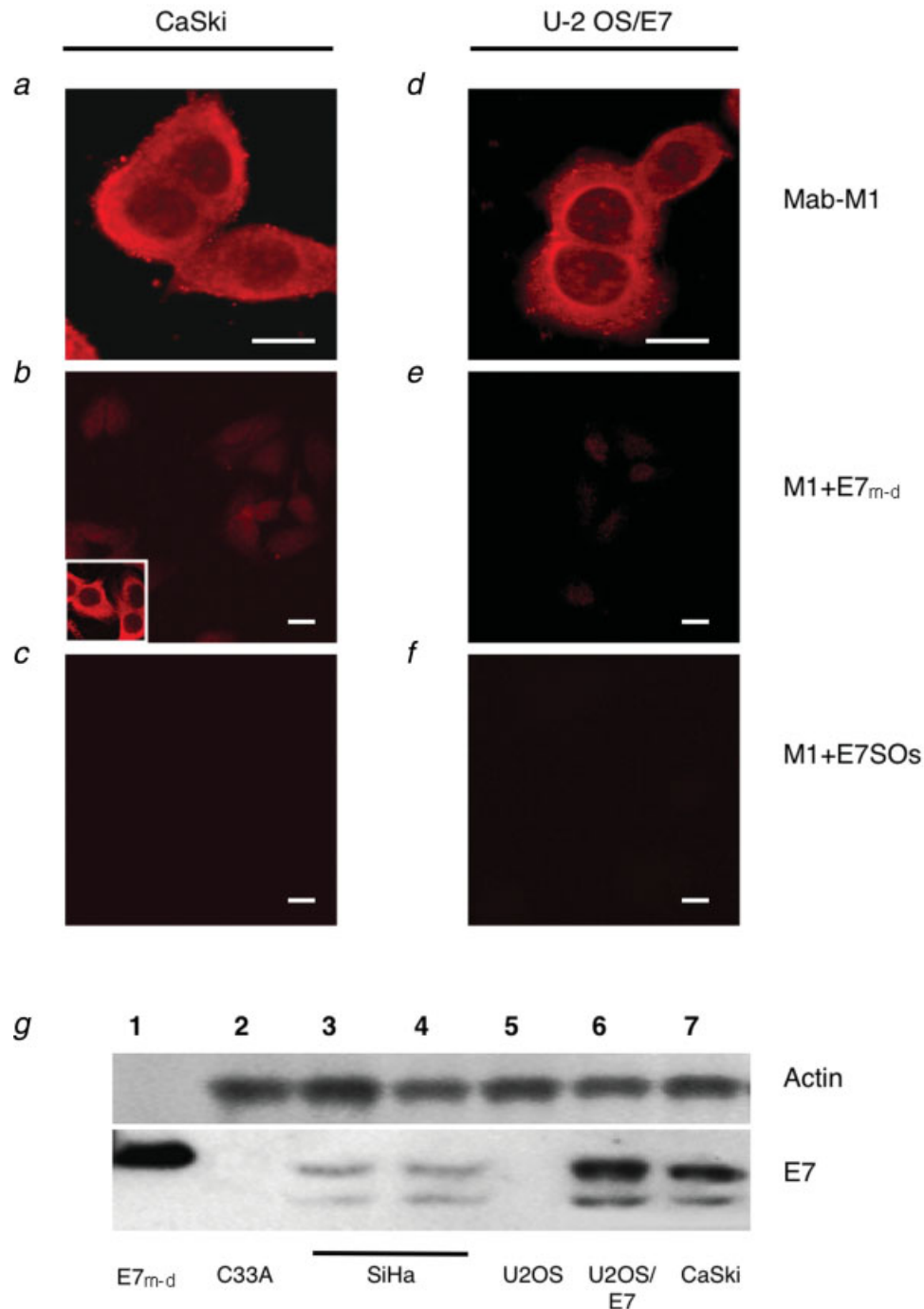


**FIGURE 3** – Localization of HPV-16 E7 in HPV-linked carcinoma cell lines. CaSki (*a–c*), and E7 transfected U-2 OS cells (See legend for Fig. 3, *d–f*), were processed for fluorescence microscopy. Cells were stained with anti-E7 M1 monoclonal antibody (*a, d*). M1 was neutralized with purified E7<sub>m-d</sub> (*b, e*) or with E7SOs (*c, f*) prior to immunostaining. Inset in *b*: immunodepletion of nuclear signal in anti-E7SOs by E7<sub>m-d</sub> (image *e* from Fig. 1). Immunoblot of cell extracts with M1 anti-E7 antibody (*g*). Cellular proteins were separated by SDS-PAGE and blotted with M1 or anti-actin monoclonal antibodies. Lane 1: 10 ng of recombinant and purified E7, Lane 2 to 7: 10 µg of total cellular proteins of non-transfected C33A; SiHa (20 and 10 µg respectively); non-transfected U-2 OS; CaSki and transiently transfected U-2 OS with HPV16 E7. Similar results were obtained using anti-E7<sub>m-d</sub> and anti-E7SOs antibodies (not shown). [Color figure can be viewed in the online issue, which is available at [www.interscience.wiley.com](http://www.interscience.wiley.com).]

## Discussion

In our work, we set out to investigate the existence and distribution of different conformers of E7 in different cell types, and developed specific immunological tools for this purpose. We focused on the endogenous E7 protein from model HPV trans-

formed cell lines and used oligomer specific antibodies. These, in combination with immunodepletion, allowed us to determine that the oligomeric species localizes in the cytosol, while E7<sub>m-d</sub> localizes in the nucleus. This observation is strengthened by the fact that several different cell lines yield an identical result: CaSki, TC-1 and U-2 OS cells transiently transfected with HPV16 E7.

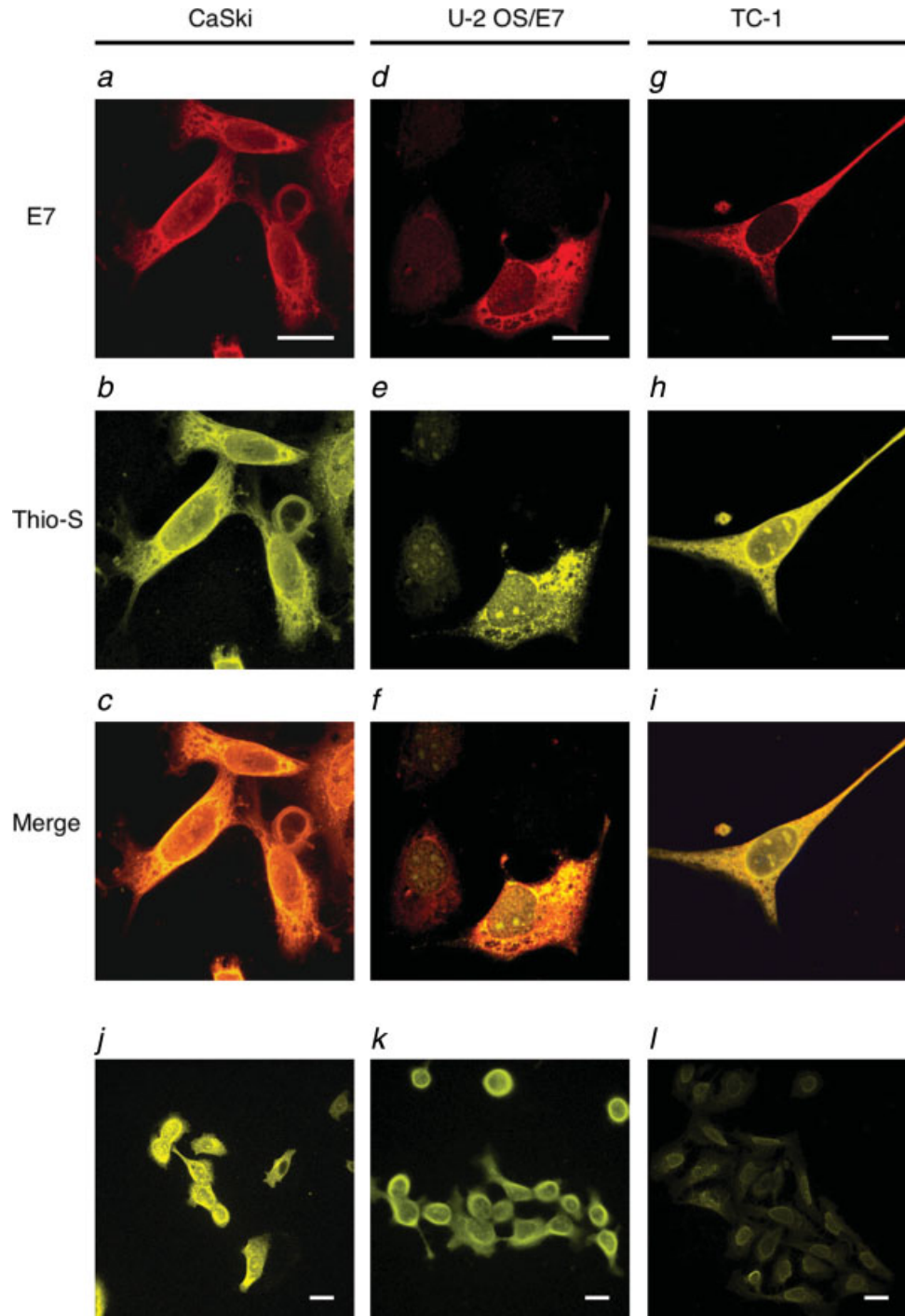


**FIGURE 4** – Amyloid-like properties of cytosolic HPV16 E7. CaSki (*a–c*), transiently transfected U-2 OS/E7 (*d–f*), and TC-1 (*g–i*) cell lines were co-stained with anti-E7 M1 antibody (red) and thioflavin-S dye (yellow). The merged images of E7 and thioflavin-S are shown in orange. Low magnification of thioflavin-S staining of CaSki (*j*) and U-2 OS/E7 (*k*) are shown. (*l*) Untransfected U-2 OS cells were analyzed for thioflavin-S labeling as control. The colocalization coefficient is shown in supplemental material. Bar: 10  $\mu$ m.

The anti-E7 M1 monoclonal does not discriminate conformers but detects higher levels of E7 in the cytosol, strongly suggesting that oligomeric species are indeed the most abundant.

It has been reported that E7 is a predominantly nuclear protein either in naturally transformed cell lines as CaSki, or in experimental human cell lines transiently transfected with an expressing fused or non-fused E7.<sup>29</sup> Others have described a cytoplasmic localization<sup>30,31</sup> and an association of a GFP tagged E7 to the nuclear matrix.<sup>16</sup> Recently, E7 has been detected in cytosol as well as in the nucleus of cervical cancer smears with polyclonal antisera.<sup>32</sup> All cases referred to the *total* E7 pool.

The amyloid-like nature of the cytosolic oligomers was confirmed by a strong co-localization of thioflavin-S staining with that of E7 in immunofluorescence. We cannot determine the precise nature of the oligomers, but we believe they may be homo-oligomers or hetero-oligomers resulting from the association of E7 with many of the different cytosolic targets described. Once again, this was confirmed in the 3 different HPV E7 containing cell models. In addition, amyloid is a conformation potentially attainable by most proteins and can be either toxic as in neurodegenerative diseases<sup>33</sup> or functional, as recently described.<sup>34</sup> In any case, the detection of amyloid-like oligomers specifically located

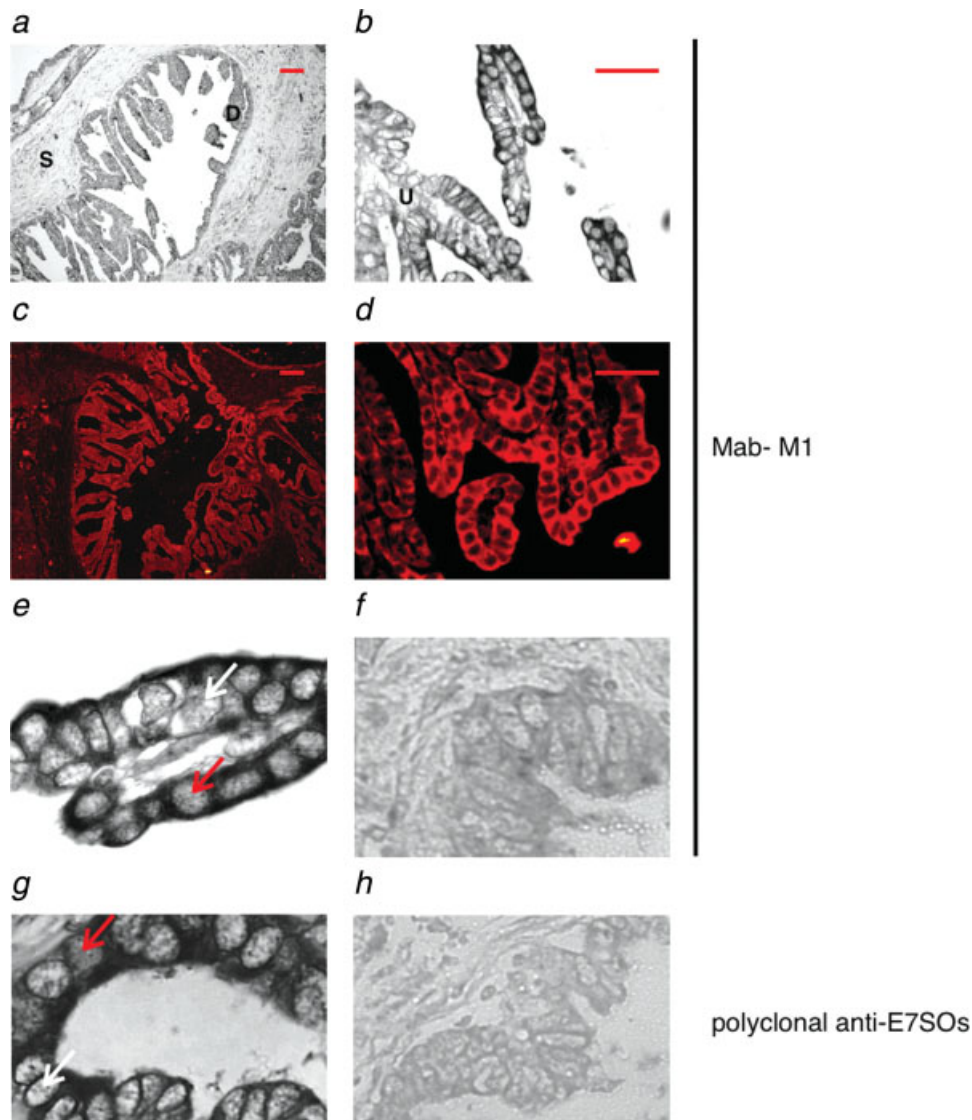


**FIGURE 5** – Immunohistochemical staining of biopsies of high-risk HPV16-positive endometrioid adenocarcinoma. Immunoperoxidase and Cy3 staining of the paraffin sections of the carcinoma with M1 anti-E7 (a–e) or with the polyclonal anti-E7SOs purified gamma fraction (g). Controls: paraffin sections of the same tissue stained by anti-E7 M1 (f) or anti-E7SOs (h) immunodepleted by preincubation with purified HPV-16 E7SOs. (e and g) Larger magnifications of the staining for a more detailed comparison of the localization by the two antibodies. Bars: 10  $\mu$ M. Red arrow: nucleus positive for E7 label; white arrow: nucleus with no labeling. S, Stroma; D, differentiated area; U, undifferentiated area. [Color figure can be viewed in the online issue, which is available at [www.interscience.wiley.com](http://www.interscience.wiley.com).]

in the cell support the hypothesis that at some stage, E7 may act as a chaperone-holdase or “sticky protein” by interacting with a number of varied cell targets.<sup>24</sup> Amyloid staining is not detectable in the nuclei, coincident with the lack of thioflavin-S binding by the E7<sub>m-d</sub>.<sup>23</sup>

Biopsy specimens of HPV related cancerous tissue show a strong label of E7, with a mild signal in the nucleus and a strong cytoplasmic localization, in excellent agreement with the 3 different model cell lines described. Close inspection of staining with anti-E7SOs, shows a remarkable coincidence with anti-E7 M1 monoclonal, providing a strong indication that oligomeric E7 species exists mainly in cytosol of cancerous cells. This strong E7 localization is found exclusively in differentiated regions of the carcinoma, in agreement with observations which showed that the E7 protein drives S-phase reentry in post-mitotic, differentiated keratinocytes in raft cultures.<sup>35</sup>

To our surprise, the cytosolic oligomers are not static and can be imported into the nucleus when the nuclear E7<sub>m-d</sub> pools are

degraded. Given the size of the nuclear pore, we assume that the oligomers must be disassembled somehow, and this takes place within a few hours. The fact that E7<sub>m-d</sub> localizes into the nucleus strongly suggests that this is the species that promotes pRb degradation.<sup>12,27,28</sup>

Using N-terminus GFP tagging in transfected HeLa cells, HPV16 E7 was shown to localize only in the nucleus, and a non-classical ran-dependent import pathway was proposed.<sup>29</sup> However, total E7 was shown to be short-lived and degraded by the proteasome through ubiquitination at its N-terminus.<sup>18,36</sup> In fact, a lysine less HPV 58 E7 was shown to be one of the few proteins that are ubiquitinated at the N-terminus.<sup>17</sup> Thus, blocking the N-terminus of E7 will extend the half-life of the oncoprotein. Moreover, given that E7 is a promiscuous binder, over-expression of the protein and co-immune precipitation of concentrated extracts may lead to the large number of candidate targets reported.<sup>22</sup> We share the view of Kalejta, in that multifunctional oncoproteins from DNA tumor viruses with small genomes could be described as “a bull in a china shop.”<sup>13</sup>



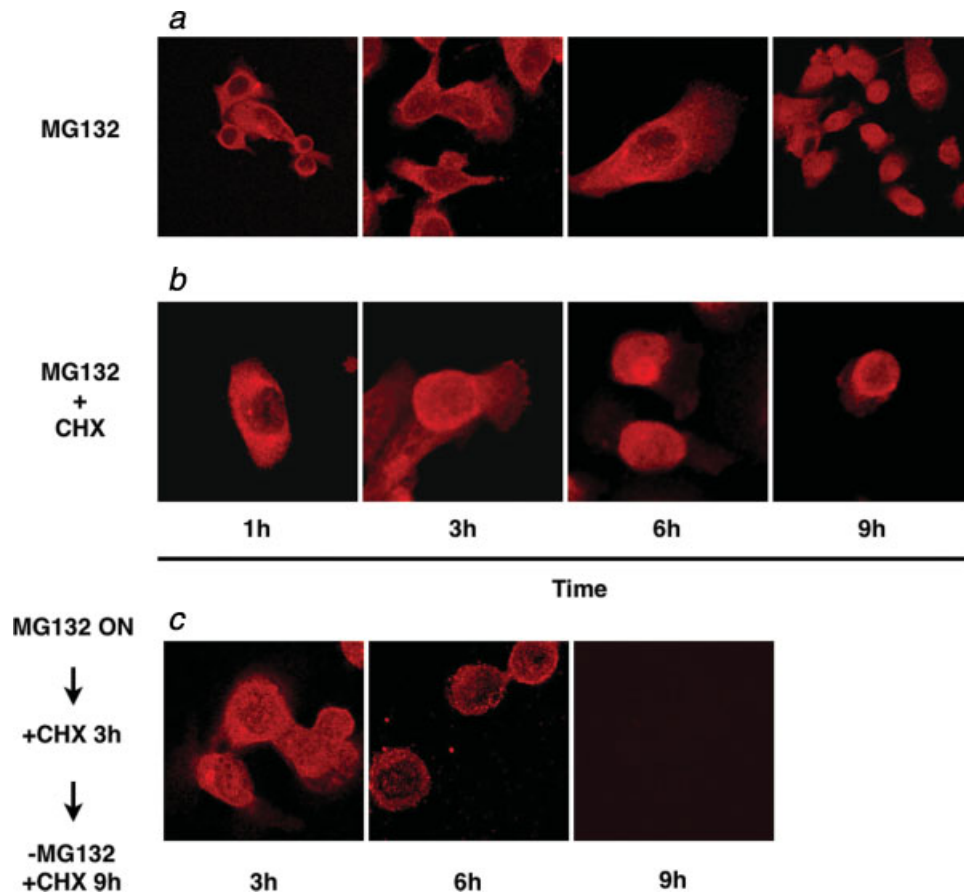


**FIGURE 6** – The oligomeric cytosolic pool of E7 is dynamic. Time course E7 nuclear accumulation induced in CaSki by proteasome inhibition (a). Cells were treated with 10 μM of MG132 for 9 hr. Cells were fixed at the indicated times and stained by the M1 antibody. Cells were treated simultaneously for the inhibition of protein synthesis and proteasomal degradation using 1 μM of cycloheximide and 10 μM of MG132, respectively (b). Cells were pre-treated with MG132 for 14 hr followed by the addition of CHX, after 3 hr of treatment, cells were washed with CHX only (c). [Color figure can be viewed in the online issue, which is available at [www.interscience.wiley.com](http://www.interscience.wiley.com).]

The chaperone-holdase activity of E7SOs<sup>24</sup> may explain a non-specific binding activity that may affect many different targets, some of which can lead to irreversible transformation. In fact, small and large T antigens of SV40 virus were shown to be molecular chaperones, with key roles in viral replication and tumorigenesis.<sup>37</sup>

We propose that amyloid-stained cytosolic species can be homo or hetero-oligomers of E7, bound to different targets. These can be imported to the nucleus, where E7<sub>m-d</sub> exerts its primary effect on pRb degradation. Although we cannot discriminate the half-life of the different conformers, nuclear E7 was shown to be labile, and perhaps E7<sub>m-d</sub> is only degraded in the nucleus as described by various groups.<sup>37,38</sup> Our results of cycloheximide inhibition show that the cytosolic E7 disappears between 6 and 9 hr after treatment, providing a gross estimate of a much longer half-life for the amyloid-like oligomeric forms (Fig. 5, Supporting Information).

So far, the E7 protein could not be detected in early infection models with the intact HPV genome, which strongly suggests that the protein levels are very low. However, given the high affinity for pRb or p130, low levels of E7 will suffice. Its primary effect would indeed be to target these key proteins for degradation, allowing the entrance into S phase for viral genome replication. This unique event would not *per se* cause the irreversible transformation that leads ultimately to cancer progression. In fact, HPV related cervical cancer takes years to declare.<sup>38</sup> The build up of cytosolic oligomeric E7 should be the result of uncontrolled

expression that takes place upon factors such as the integration of the viral DNA to the host genome, which disrupts the negative control on E7 expression by E2.<sup>39,40</sup> A recent report indicates that integration of the HPV genome occurs at a large number of sites, with consequences on the level of expression of the oncoproteins, depending on the adjacent promoters.<sup>41</sup> However, we cannot rule out the possibility that the monomeric/dimeric form is modified in the nucleus and rapidly transported and degraded into the cytoplasm.

Additional, yet, unknown long-term events which may inhibit E7's repression or risk factors, may contribute to the increase of E7 expression prior or in parallel with genome integration. Excess of E7 would accumulate in the cytosol in the form of the oligomers we describe, with the ability to bind several different targets. Some of these interactions will be innocuous and others may lead to an irreversible progression into carcinogenesis. The large list of potential E7 binders include pocket proteins, transcription factors, chromatin remodeling proteins, negative regulators of the cell cycle and components of the innate immune response and cytoskeletal proteins, but the list is larger.<sup>22,30,42,43</sup> Many of these proteins are located in the cytosol, such as those involved in destabilization of centrosomes that leads to mitotic defects and genome instability.<sup>44</sup> In the case of transcription factors or proteins that act within the nucleus, accumulated cytosolic E7 may interfere with their import into this compartment after synthesis, and thus interfere with their key regulatory functions.

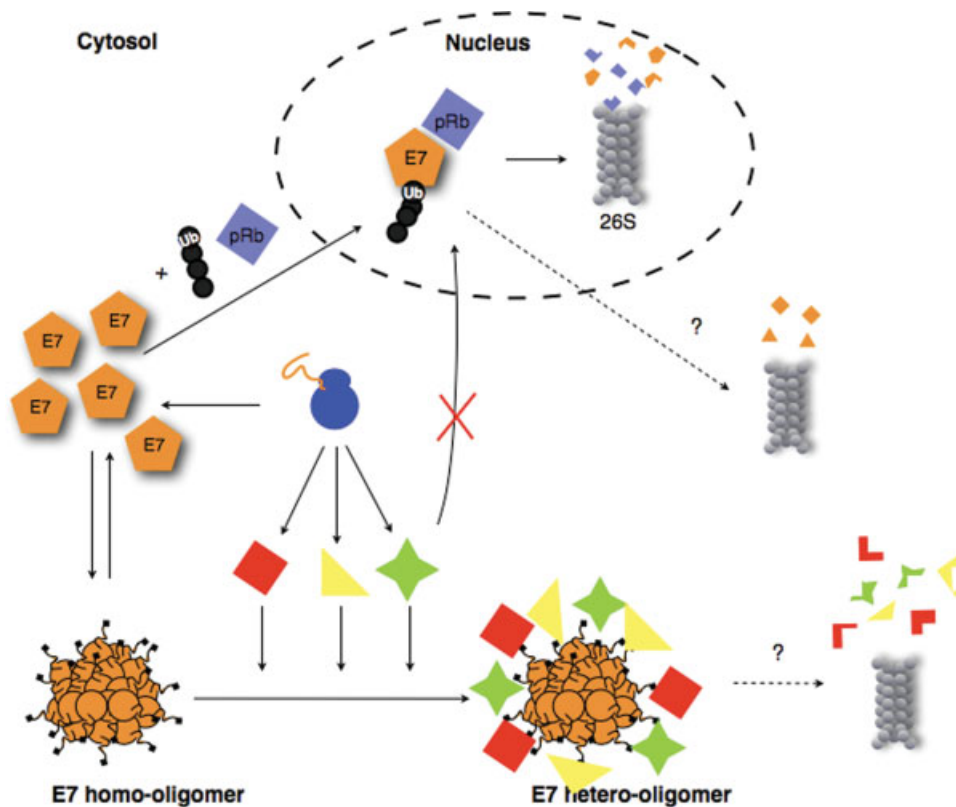


**FIGURE 7** – Model for the cellular distribution of endogenous high-risk E7 conformers in cells (see Discussion). [Color figure can be viewed in the online issue, which is available at [www.interscience.wiley.com](http://www.interscience.wiley.com).]

Figure 7 summarizes the model we propose based on the results presented here. The model, including the localization of monomeric and oligomeric E7 conformers, resembles the situation of endogenous E6 in CaSki and HeLa cells.<sup>45</sup> As it is known, E6 will cooperate in early transformation by targeting p53 and later participating in loss of cell adhesion and polarity, thus contributing to malignancy.<sup>42,46</sup>

The existence of different conformers of E7 raises new questions to be addressed concerning the operating mechanisms in tissues that appear to go beyond the promotion of pRb and pocket protein degradation. In addition, it should be established which E7 species are undetectable by immune surveillance and which are antigenic, provided the need and ongoing development of therapeutic vaccines.<sup>47</sup> Finally, there are a few examples regarding a connection between amyloids and tumorigenesis. One, the formation of intracellular amyloid fibers in Bence Jones -type myeloma,<sup>48</sup> the directly related to HPV: a localized amyloidosis in endometrioid adenocarcinoma,<sup>49</sup> and recently, the report of an amyloid-like form of 16E1E4 which explains its accumulation during productive infection and its effect on cellular integrity.<sup>50</sup>

What is becoming clear is that at least 4 human genes appear to have a dual role: 1 in amyloid related neurodegeneration and the other in cell-cycle control, where both roles are proposed to be the 2 sides of the same coin.<sup>51</sup>

#### Note Added in Proof

It recently came to our knowledge a report that shows HPV16 E7 localized in the cytosol, ER, golgi, and in the nucleus of CaSki cells.<sup>52</sup>

#### Acknowledgements

Ms. Karina I. Dantur is a recipient of a Florencio Florini Fellowship, from the Argentine National Academy of Medicine. We thank Ms. Lucía Chemes for critical reading of the manuscript and Ms. Vanesa Gottifredi for valuable comments. Mr. Leonardo G. Alonso, Mr. Eduardo M. Castaño, Ms. Laura Morelli and Mr. Gonzalo de Prat Gay are Career Investigators from CONICET.

#### References

- Kim HY, Ahn BY, Cho Y. Structural basis for the inactivation of retinoblastoma tumor suppressor by SV40 large T antigen. *EMBO J* 2001;20:295–304.
- Barbosa MS, Edmonds C, Fisher C, Schiller JT, Lowy DR, Vousden KH. The region of the HPV E7 oncoprotein homologous to adenovirus E1a and Sv40 large T antigen contains separate domains for Rb binding and casein kinase II phosphorylation. *EMBO J* 1990;9:153–60.
- Dyson N, Guida P, McCall C, Harlow E. Adenovirus E1A makes two distinct contacts with the retinoblastoma protein. *J Virol* 1992;66:4606–11.
- Genovese NJ, Banerjee NS, Broker TR, Chow LT. Casein kinase II motif-dependent phosphorylation of human papillomavirus E7 protein promotes p130 degradation and S-phase induction in differentiated human keratinocytes. *J Virol* 2008;82:4862–73.
- Munger K, Baldwin A, Edwards KM, Hayakawa H, Nguyen CL, Owens M, Grace M, Huh K. Mechanisms of human papillomavirus-induced oncogenesis. *J Virol* 2004;78:11451–60.
- zur Hausen H. Papillomaviruses causing cancer: evasion from host-cell control in early events in carcinogenesis. *J Natl Cancer Inst* 2000;92:690–8.
- Harper DM, Franco EL, Wheeler CM, Moscicki AB, Romanowski B, Roteli-Martins CM, Jenkins D, Schuind A, Costa Clemens SA, Dubin G. Sustained efficacy up to 4.5 years of a bivalent L1 virus-like particle vaccine against human papillomavirus types 16 and 18: follow-up from a randomised control trial. *Lancet* 2006;367:1247–55.

8. Frazer I. Vaccines for papillomavirus infection. *Virus Res* 2002;89: 271–4.
9. Howley PM, Lowy R. Papillomaviruses and their replication. In: Knipe D, Howley PM, eds. *Fields in virology*. Philadelphia: Lippincott Williams and Wilkins, 2001. 2197–229.
10. Munger K, Phelps WC, Bubbs V, Howley PM, Schlegel R. The E6 and E7 genes of the human papillomavirus type 16 together are necessary and sufficient for transformation of primary human keratinocytes. *J Virol* 1989;63:4417–21.
11. Scheffner M, Werness BA, Huibregtse JM, Levine AJ, Howley PM. The E6 oncoprotein encoded by human papillomavirus types 16 and 18 promotes the degradation of p53. *Cell* 1990;63:1129–36.
12. Boyer SN, Wazer DE, Band V. E7 protein of human papilloma virus-16 induces degradation of retinoblastoma protein through the ubiquitin-proteasome pathway. *Cancer Res* 1996;56:4620–4.
13. Kalejta RF. Human cytomegalovirus pp71: a new viral tool to probe the mechanisms of cell cycle progression and oncogenesis controlled by the retinoblastoma family of tumor suppressors. *J Cell Biochem* 2004;93:37–45.
14. Narisawa-Saito M, Kiyono T. Basic mechanisms of high-risk human papillomavirus-induced carcinogenesis: roles of E6 and E7 proteins. *Cancer Sci* 2007;98:1505–11.
15. Fiedler M, Muller-Holzner E, Viertler HP, Widschwendter A, Laich A, Pfister G, Spoden GA, Jansen-Durr P, Zwierschke W. High level HPV-16 E7 oncoprotein expression correlates with reduced pRb-levels in cervical biopsies. *FASEB J* 2004;18:1120–2.
16. Greenfield I, Nickerson J, Penman S, Stanley M. Human papillomavirus 16 E7 protein is associated with the nuclear matrix. *Proc Natl Acad Sci USA* 1991;88:11217–21.
17. Ben-Saadon R, Fajerman I, Ziv T, Hellman U, Schwartz AL, Ciechanover A. The tumor suppressor protein p16(INK4a) and the human papillomavirus oncoprotein-58 E7 are naturally occurring lysine-less proteins that are degraded by the ubiquitin system. Direct evidence for ubiquitination at the N-terminal residue. *J Biol Chem* 2004;279: 41414–21.
18. Reinstein E, Scheffner M, Oren M, Ciechanover A, Schwartz A. Degradation of the E7 human papillomavirus oncoprotein by the ubiquitin-proteasome system: targeting via ubiquitination of the N-terminal residue. *Oncogene* 2000;19:5944–50.
19. Clemens KE, Brent R, Gyuris J, Munger K. Dimerization of the human papillomavirus E7 oncoprotein in vivo. *Virology* 1995;214: 289–93.
20. Liu X, Clements A, Zhao K, Marmorstein R. Structure of the human papillomavirus E7 oncoprotein and its mechanism for inactivation of the retinoblastoma tumor suppressor. *J Biol Chem* 2006;281:578–86.
21. Alonso LG, Garcia-Alai MM, Nadra AD, Lapena AN, Almeida FL, Gualfetti P, Prat-Gay GD. High-risk (HPV16) human papillomavirus E7 oncoprotein is highly stable and extended, with conformational transitions that could explain its multiple cellular binding partners. *Biochemistry* 2002;41:10510–8.
22. Munger K, Howley PM. Human papillomavirus immortalization and transformation functions. *Virus Res* 2002;89:213–28.
23. Alonso LG, Garcia-Alai MM, Smal C, Centeno JM, Iacono R, Castano E, Gualfetti P, Prat Gay Gd. The HPV16 E7 viral oncoprotein self-assembles into defined spherical oligomers. *Biochemistry* 2004;43:3310–7.
24. Alonso LG, Smal C, Garcia-Alai MM, Chemes L, Salame M, Prat Gay Gd. Chaperone holdase activity of human papillomavirus E7 oncoprotein. *Biochemistry* 2006;45:657–67.
25. Galfre G, Milstein C. Preparation of monoclonal antibodies: strategies and procedures. *Methods Enzymol* 1981;73:3–46.
26. Lin KY, Guarnieri FG, Staveley-O'Carroll KF, Levitsky HI, August JT, Pardoll DM, Wu TC. Treatment of established tumors with a novel vaccine that enhances major histocompatibility class II presentation of tumor antigen. *Cancer Res* 1996;56:21–6.
27. Gonzalez SL, Stremlau M, He X, Basile JR, Munger K. Degradation of the retinoblastoma tumor suppressor by the human papillomavirus type 16 E7 oncoprotein is important for functional inactivation and is separable from proteasomal degradation of E7. *J Virol* 2001;75:7583–91.
28. Wang J, Sampath A, Raychaudhuri P, Bagchi S. Both Rb and E7 are regulated by the ubiquitin proteasome pathway in HPV-containing cervical tumor cells. *Oncogene* 2001;20:4740–9.
29. Angeline M, Merle E, Moroianu J. The E7 oncoprotein of high-risk human papillomavirus type 16 enters the nucleus via a nonclassical Ran-dependent pathway. *Virology* 2003;317:13–23.
30. Rey O, Lee S, Baluda MA, Sweet J, Ackerson B, Chiu R, Park NH. The E7 oncoprotein of human papillomavirus type 16 interacts with F-actin in vitro and in vivo. *Virology* 2000;268:372–81.
31. Smotkin D, Wettstein FO. The major human papillomavirus protein in cervical cancers is a cytoplasmic phosphoprotein. *J Virol* 1987;61:1686–9.
32. Jeon JH, Shin DM, Cho SY, Song KY, Park NH, Kang HS, Kim YD, Kim IG. Immunocytochemical detection of HPV16 E7 in cervical smear. *Exp Mol Med* 2007;39:621–8.
33. Comenzo R. Amyloidosis. *Curr Treat Options Oncol* 2006;7:225–36.
34. Fowler DM, Koulov AV, Balch WE, Kelly JW. Functional amyloid—from bacteria to humans. *Trends Biochem Sci* 2007;32:217–24.
35. Banerjee NS, Genovese NJ, Noya F, Chien WM, Broker TR, Chow LT. Conditionally activated E7 proteins of high-risk and low-risk human papillomaviruses induce S phase in postmitotic, differentiated human keratinocytes. *J Virol* 2006;80:6517–24.
36. Oh KJ, Kalinina A, Wang J, Nakayama K, Nakayama KI, Bagchi S. The papillomavirus E7 oncoprotein is ubiquitinated by UbcH7 and Cullin 1- and Skp2-containing E3 ligase. *J Virol* 2004;78:5338–46.
37. Sullivan CS, Pipas JM. T antigens of simian virus 40: molecular chaperones for viral replication and tumorigenesis. *Microbiol Mol Biol Rev* 2002;66:179–202.
38. Schiller JT. Chapter 17: Second generation HPV vaccines to prevent cervical cancer. *Vaccine* 2006;24 (Suppl 3):S147–53.
39. Pett MR, Alazawi WO, Roberts I, Dowen S, Smith DI, Stanley MA, Coleman N. Acquisition of high-level chromosomal instability is associated with integration of human papillomavirus type 16 in cervical keratinocytes. *Cancer Res* 2004;64:1359–68.
40. Romanczuk H, Howley PM. Disruption of either the E1 or the E2 regulatory gene of human papillomavirus type 16 increases viral immortalization capacity. *Proc Natl Acad Sci USA* 1992;89:3159–63.
41. Kraus I, Driesch C, Vinokurova S, Hovig E, Schneider A, von Knebel Doeberitz M, Durst M. The majority of viral-cellular fusion transcripts in cervical carcinomas cotranscribe cellular sequences of known or predicted genes. *Cancer Res* 2008;68:2514–22.
42. Campo S. The essential transforming proteins of HPV: E5, E6 and E7. *HPV Today Publ* 2005:8–10.
43. Howley PM, Munger K, Romanczuk H, Scheffner M, Huibregtse JM. Cellular targets of the oncoproteins encoded by the cancer associated human papillomaviruses. *Princess Takamatsu Symp* 1991;22:239–48.
44. Duensing S, Munger K. Human papillomaviruses and centrosome duplication errors: modeling the origins of genomic instability. *Oncogene* 2002;21:6241–8.
45. Garcia-Alai MM, Dantur KI, Smal C, Pietrasanta L, Prat Gay GD. High-risk HPV E6 oncoproteins assemble into large oligomers that allow localization of endogenous species in prototypic HPV-transformed cell lines. *Biochemistry* 2007;46:341–9.
46. Thomas M, Pim D, Banks L. The role of HPV E6 oncoprotein in malignant progression. In: Campo SM, ed. *Papillomavirus research: from natural history to vaccines and beyond*. England: British Library Cataloguing in publication data, 2006.115–31.
47. Hung CF, Ma B, Monie A, Tsen SW, Wu TC. Therapeutic human papillomavirus vaccines: current clinical trials and future directions. *Expert Opin Biol Ther* 2008;8:421–39.
48. Nomura S, Kanoh T, Uchino H. Intracellular formation of amyloid fibrils in myeloma. Cytochemical, immunochemical, and electron microscopic observations. *Cancer* 1984;54:303–7.
49. Kotru M, Manucha V, Singh UR. Cytologic and histologic features of primary mucinous adenocarcinoma of skin in the axilla: a case report. *Acta Cytol* 2007;51:571–4.
50. McIntosh PBMS, Jackson DJ, Khan J, Isaacson ER, Calder L, Raj K, Griffin HM, Wang Q, Laskey P, Eccleston JF, Doorbar J. Structural analysis reveals an amyloid form of the HPV 16 E1E4 protein and provides a molecular basis for its accumulation. *J Virol* 2008;16:8196–203.
51. Staropoli JF. Tumorigenesis and neurodegeneration: two sides of the same coin? *Bioessays* 2008;30:719–27.
52. Valdovinos-Torres H, Orozco-Morales M, Pedroza-Saavedra A, Padilla-Noriega A, Esquivel-Guadarrama F, Gutierrez-Xicotencatl L. Different isoforms of HPV-16 E7 protein are present in cytoplasm and nucleus. *J Open Virol* 2008;2:15–23.